Detection of Gap Mura in TFT LCDs by the Interference Pattern and Image Sensing Method

Jang Zern Tsai, Rong-Seng Chang, and Tung-Yen Li

***Abstract*—In this paper, we focus on pretesting to find the gap mura defects before the injection of liquid crystal into the cell of a thin-film-transistor liquid-crystal display panel. An optical interference pattern sensing method for inspection of the gap mura defects is used. We propose automatic quantization of mura panel defects in terms of the crossing points of the interference pattern. By doing so, panels with unacceptable gap mura could be sorted out simply by a binary classification, which facilitates automated visual inspection. The advantages of using this method include that it allows for pretesting before the injection of liquid crystal, meaning that defective panels can be found before the next process step and the wastage of liquid crystal materials can be avoided. The yield rate and manufacturing process efficiency can be improved and the inspection time can be shortened from 20 s by human inspection to less than 2 s by automatic inspection. Experiment results show that the proposed method offers improved performance for gap mura detection.**

***Index Terms*—I/Image classification, I/Image processing, L/Liquid crystal displays, L/Liquid crystals, O/Optical signal detection.**

I. Introduction

MURA are visible defects that appear as local variations in lightness variation with low contrast and nonuniform brightness on a thin film transistor liquid crystal display (TFT LCD). They are often larger than one pixel and without fixed area and shape. A mura defect can be defined as any region that is darker or lighter than other places on the surface of TFT LCDs. Mura defects are caused during the manufacturing process of TFT LCD panels. They usually have unclear boundaries and are hard to recognize in the unfinished product. To sort out defective panels during the manufacturing process, the factory manager may arrange operators to inspect the panels and pick out the ones they see are defective. However, this is a subjective process and the quality depends on the skill of the human operators.

Manuscript received September 12, 2012; revised February 20, 2013; accepted February 23, 2013. Date of publication July 9, 2013; date of current version October 7, 2013. This work was supported part by the National Science Council of Taiwan under Grant NSC-97-2218-E-008-001. The Associate Editor coordinating the review process was Shervin Shirmohammadi (*Corresponding author: T.-Y. Li*).

J.-Z Tsai and T.-Y. Li are with the Department of Electrical Engineering, National Central University, Jung-Li City 320, Taiwan (e-mail: jztsai@ee.ncu.edu.tw; ligalike@gmail.com).

R.-S. Chang is with the Department of Optics and Photonics, National Central University, Jungg-Li City 320, Taiwan (e-mail: rschang2011@gmail.com).

Color versions of one or more of the figures in this paper are available online at http://ieeexplore.ieee.org.

Digital Object Identifier 10.1109/TIM.2013.2270049

There are many kinds of mura defects, including lines, blobs, gaps etc. Gap mura defects have low contrast and unclear contours, making them more difficult to recognize than other types of defects. Mura defects can be caused by photo-mask problems, inconsistent particle size, roughness of the glass surface, low quality liquid crystal, polarizer nonuniformity, bad process control, and so on.

There have been some studies about mura detection [1]–[4]. Recently, Tseng proposed a mura detection method that integrated the techniques of multiimage accumulation and multiresolution background subtraction [5]. Bi presented a method for machine vision inspection [6] by combining the level set method and real Gabor filters for the detection of mura defects. Taniguchi applied the image processing and quantity flow techniques with the shadow mask and edge mask method to make the judgment of the image more correct [7].

In this paper, we concentrated on developing an effective method for gap mura defect inspection. The TFT LCD manufacturing process depends on the mounting of two glass sheets with sealant around the four sides. The sealant is dispensed from syringes leaving a very narrow space called the cell gap between the two sheets, which is then filled with liquid crystal. However, as we know, the two plates of glass are not perfectly uniform and may not be perfectly parallel to each other. Some unexpected situations could occur during the manufacturing process of the LCD panel. The three main causes of gap mura defect are: nonuniformity of the sealant around the panel, foreign materials in the panel and the presence of a fiber-cluster at the edge of the panel.

On the production line, operators are trained to inspect panels by the human eye. However, this method of defect detection is primarily dependent upon personal experience and subjective judgment, and consistency of the inspection standards can be a problem, which often affects the test results. More importantly, the inspection method currently used in the production line and the methods described in those previous research works mentioned above can only test finished LCD panels, which cannot prevent bad panel production.

Reduction of the yield loss could lead to savings on manufacturing costs. It is thus important to find an easy and quick method to detect these mura defects. For this purpose, an interference pattern [8]–[10] and a statistical measurement method (the binary classification method) are introduced in this paper, which offers faster inspection for the detection of mura defects.

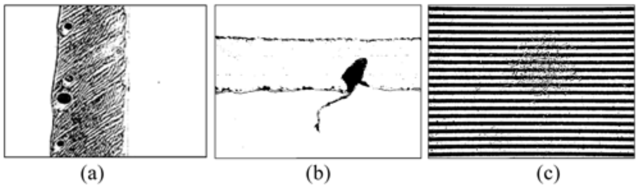

Fig. 1. Different sealant problems that can cause mura defects. (a) Non-uniformity of the sealant around the panel. (b) Foreign materials in the panel. (c) Fiber-cluster at the edge of the panel.

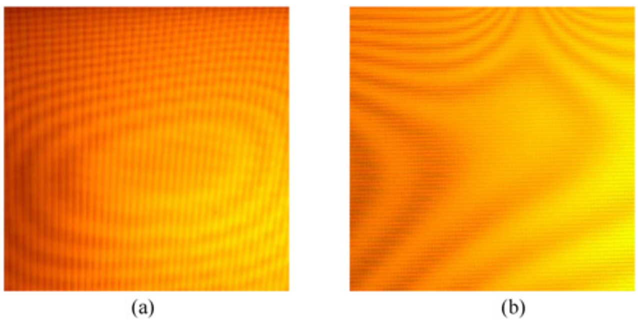

Fig. 2. (a) Normal Interference patterns. (b) Abnormal Interference patterns on TFT LCDs under sodium light.

Our novel method focuses on the pretesting process. The assumption is that if gap mura defects in the panels can be sorted out during the inspection procedure before the injection of the liquid crystal into the cell of the LCD panel, then the quality of the panel could be corrected in the pretest process and the wastage of liquid crystal materials that occurred later in the process could be avoided.

II. Experimental Methods

A. Interference Pattern with Two Parallel Glass Plates

There is an observable phenomenon of interference patterns that appears with two parallel glass plates separated by a very narrow space [11]. We know that the interference pattern is caused by the superposition of two or more optical waves. Under a monochromatic light source like a sodium lamp, an alternately bright (constructive interference) and dark (destructive interference) pattern appears (Fig. 2).

Fig. 3 shows two parallel planar plates of transparent material illuminated by a point source S of a monochromatic light. We suppose point P to be on the same side of the plate as point S. The two optical paths from point S to point P are represented by "$\overline{\text{SABCDEP}}$" and "$\overline{\text{SABFNP}}$".

The optical path difference ΔS can be formulated as

$$\Delta \text{S} = \overline{\text{SABCDEP}} - \overline{\text{SABFNP}} = \text{n}(\overline{\text{BC}} + \overline{\text{CD}}) - \text{n}(\overline{\text{FN}}) \quad (1)$$

where n' is the refractive index of the glass plate, n is the refractive index of the environment and h is the gap between the two planar parallel plates. We define θ and θ' as the angles of incidence and refraction at the upper surface, respectively, to obtain

$$\overline{\text{BC}} = \overline{\text{CD}} = \frac{\text{h}}{\cos\theta} \quad (2)$$

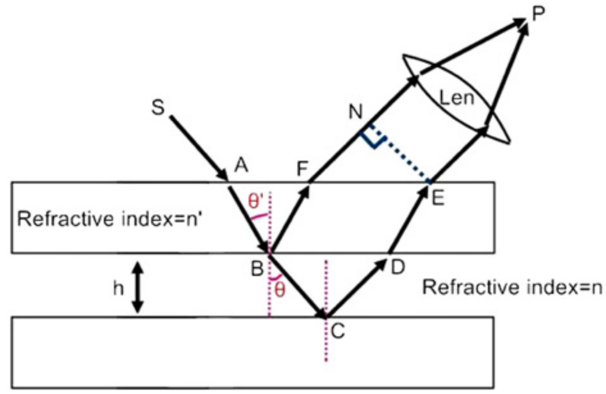

Fig. 3. Light path of point source S through planar parallel plates.

and

$$\overline{\text{FN}} = \overline{\text{EF}} \sin\theta = 2\text{h} \times \tan\theta \times \sin\theta. \quad (3)$$

According to Snell's law,

$$n' \sin\theta' = n \sin\theta. \quad (4)$$

Thus, from (1) to (4), we can get

$$\Delta S = \frac{2nh}{\cos\theta} - 2nh \times \tan\theta \times \sin\theta = 2nh, \cos\theta \quad (5)$$

and the phase difference δ is

$$\delta = \left(\frac{2\pi}{\lambda_0}\right) \times \Delta S = \left(\frac{4\pi}{\lambda_0}\right) nh\cos\theta, \quad (6)$$

where λ0 is the wavelength of light in the glass plate.

Angle θ is determined by point P on the focal plane of a CCD Camera, so δ is dependent on the position of S. It follows that the fringes are just distinct with an extended source such as with a point source. Since this is for one particular plane of observation, the fringes are called localized.

In general, the attitude in the pattern varies according to (5) and (6), to obtain

$$2nh\cos\theta \pm (\frac{\lambda_0}{2}) = m\lambda_0, m = 1, 2, 3... \quad (7)$$

In (7), the fringe patterns are brightened

$$2nh\cos\theta \pm (\frac{\lambda_0}{2}) = m\lambda_0, m = \frac{1}{2}, \frac{3}{2}, \frac{5}{2}... \quad (8)$$

In (8), the fringe patterns are darkened.

An interference fringe is characterized by a value θ and is formed by a ray incident on the plate. For this reason, the fringes are called fringes of equal inclination. When θ and θ' are equal to zero, the fringes appear as concentric circles. The interference is the highest at the center of the pattern. When h increases, the fringes expand from the center of the pattern. A new fringe appears each time h increases by $\lambda_0/2$ (n = 1 for air).

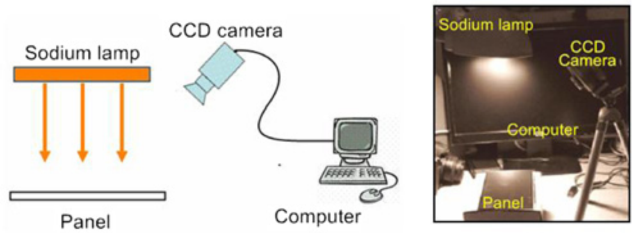

Fig. 4. Photo of the interference pattern analysis system. A CCD camera is used to capture the panel image.

B. Experiment Equipment

Fig. 4 shows the interference fringe analysis system. To facilitate the identification of interference fringes, a monochromatic sodium light source with a wavelength of 550-600 nm (obtained from Ying Mao Industry FNA-35S, Taipei, Taiwan) was used. This created alternate bright and dark concentric rings which made it easier to detect defects. This kind of light source is commonly used to assess LCD panels in terms of coating thickness and surface flatness. A CCD camera (Canon IXUS 210 / 14 Megapixels, Japan) is used to capture images of the fringes on the panel, followed by image processing software to enhance the fringe images before further analysis.

C. Experiment Methodology

We developed a method to overcome the problem of using subjective methods to inspect for abnormal interference patterns on LCD panels based upon finding the different interference patterns indicative of good panels and bad panels. The proposed computer aided method utilized different interference patterns to quantize the gap mura on the panels. The panels could thus be automatically classified to shorten the human inspection time. The analysis procedure is discussed below (Fig. 5). We prepared fifteen seven-inch panels without liquid crystal to be evaluated. Before evaluation, the fifteen panels were judged by an experienced operator according to the gold standard. In fact, ten panels out of the fifteen were found to have gap mura defects while the other five did not. The developed method was then used to test and to quantize the panels.

First, we fixed a panel with a holding jig. Next, we captured an image of the panel with the CCD camera under the monochromatic light of a sodium lamp. The image showing alternating bright and dark interference patterns was then processed with the MATLAB software. The histogram equalization method was utilized to improve the image contrast and clarify the captured image [12], [13]. Next, the captured image was converted into a binary image (black and white) by a binarization method. Then, the binary image was then transformed into a string and skeleton image by the thinning method. After image processing, the image was scanned from top to bottom, row by row, to find the crossing points for the evaluation of the panel (Fig. 6).

The fifteen panels were examined by comparison with the gold standard and a defect threshold was determined. If the number of crossing points on the panel exceeded the threshold, the panel was classified as bad panel. On the contrary, if

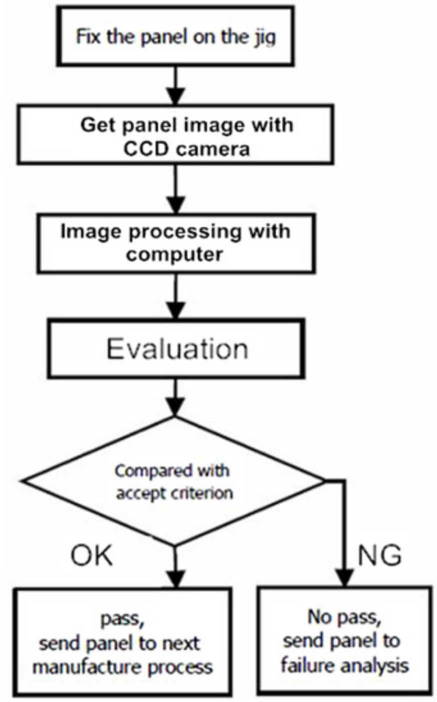

Fig. 5. Panel judging flow chart.

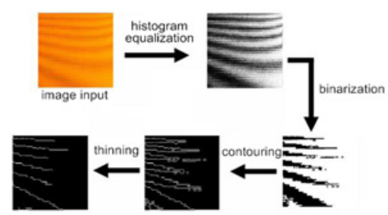

Fig. 6. Schematic of the image processing.

the number of crossing points was lower than the threshold, the panel was classified as good panel and judged to have no gap mura defects. Good panels would go on to the next manufacturing process and bad panels would go for failure analysis.

D. Definition of Crossing Points

The panel image can be divided into three groups based on the position of the defect, whether at one of the four corners, the four sides or the central area of the panel. Fig. 7 shows the diagram of a scanned area of an LCD panel and thinned interference pattern images obtained by the thinning method.

The crossing points here are defined as points crossed by the extending strings that appear in the thinned interference patterns and the panel's corners. In Fig. 7 (a), ten crossing points can be observed in the upper left-hand corner. Similarly, we can evaluate the crossing points by extending the thinned strings in comparison with the panel's sides [Fig. 7 (b)]. Seven crossing points can be found on the upper part of the panel image.

In the central area of the panel, there are concentric circles but no crossing points. In our evaluation method, we divide

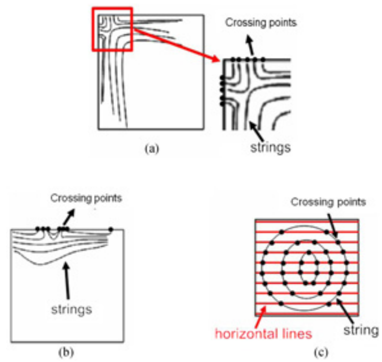

Fig. 7. (a) 5 crossing points can be observed on the top and 5 crossing points on the left side. (b) 7 crossing points can be observed on the top. (c) 35 crossing points are found in the central area.

TABLE I
COMPARE RESULTS OF THE 15 PANELS
(NOTE: "+" MEANS BAD PANEL AND "-" MEANS GOOD PANEL)

Panel no.	Total score (all cross points)	Test result of the proposed method		Operator's judgment (the gold standard)
		Threshold = 130	Threshold = 120	
1	109	–	–	Acceptable
2	104	–	–	Acceptable
3	105	–	–	Acceptable
4	105	–	–	Acceptable
5	117	–	–	Acceptable
6	121	–	+	Unacceptable
7	121	–	+	Unacceptable
8	121	–	+	Unacceptable
9	137	+	+	Unacceptable
10	140	+	+	Unacceptable
11	140	+	+	Unacceptable
12	141	+	+	Unacceptable
13	143	+	+	Unacceptable
14	143	+	+	Unacceptable
15	156	+	+	Unacceptable

the panel image into eleven parts separated by ten horizontal lines. We obtain crossing points where the horizontal lines cross the concentric circles in the thinned interference pattern [Fig. 7 (c)].

III. RESULTS AND DISCUSSION

The binary classification method was used to quantize images of ten panels with gap mura defects and five panels without gap mura defects. The acceptability criterion used a threshold, 120 points or 130 points, for determining good or bad panels. Gap mura defects were caused by differences in the distance between the panel glasses. Therefore the more interference fringes, the more different gaps it would cause, increasing the number of crossing points. When the total number of crossing points was lower than the acceptability threshold, the panel was classified as a good panel without gap mura. When the number was higher than the acceptability threshold, the panel was classified as a bad panel with gap mura. The judgment results are shown in Table I.

TABLE II
STATISTICAL RESULTS FOR A BINARY CLASSIFICATION TEST

	Unacceptable panels	Acceptable panels
Score is higher than acceptability criterion	True Positive (TP)	False Positive (FP)
Score is lower than acceptability criterion	False Negative (FN)	True Negative (TN)

The results obtained using the statistical measures from the binary classification [14], [15] test are shown in Table II: four values are defined for evaluation:

(1) True Positive (TP): Number of unacceptable panels that were detected as bad panels.
(2) False Positive (FP): Number of acceptable panels that were mistaken as bad panels.
(3) True Negative (TN): Number of acceptable panels that were detected as good panels.
(4) False Negative (FN): Number of unacceptable panels that were mistaken as good panels.

The sensitivity and specificity of the evaluated results are found and the most suitable acceptability criterion defined based on the evaluated sensitivity and specificity.

The statistical results obtained when the acceptability threshold was 130 points are shown in Fig. 8(a). $\text{Sensitivity} = TP/(TP + FN) = 7/(7 + 3) = 70\%$; $\text{Specificity} = TN/(TN + FP) = 5/(5 + 0) = 100\%$; $\text{Positive Prediction Value} = TP/(TP + FP) = 7/(7 + 0) = 100\%$ and $\text{Negative Prediction Value} = TN/(TN + FN) = 5/(5 + 3) = 62.5\%$. As can be seen in Fig. 8(a), three unacceptable panels were mistaken as good panels, but no acceptable panel was detected as bad panels. Therefore, when the acceptability criterion was 130 points, the panels could not be correctly evaluated.

The statistical results obtained when the acceptability criterion was 120 points are shown in Fig. 8(b). $\text{Sensitivity} = TP/(TP + FN) = 10/(10 + 0) = 100\%$; $\text{Specificity} = TN/(TN + FP) = 5/(5 + 0) = 100\%$; $\text{Positive Prediction Value} = TP/(TP + FP) = 10/(10 + 0) = 100\%$; $\text{Negative Prediction Value} = TN/(TN + FN) = 5/(5 + 0) = 100\%$. As can be seen in Fig. 8(b), no unacceptable panels were mistaken as good panels, and no acceptable panel was detected as bad panels. Therefore, when the acceptability criterion was 120 points, the results of automatic inspection completely conformed with the gold standard.

The sensitivity and specificity were higher when the acceptability threshold was equal to 120 points than when it was equal to 130 points. Thus, 120 is determined to be the most suitable acceptability threshold for the program to distinguish between bad and good panels.

The computer assisted detector took less than two seconds, while a human operator needed 10 - 20 seconds to check for gap mura defects. Table III shows the comparison between our and the traditional method of gap mura inspection. The traditional method can only test finished LCD panels, it cannot prevent the production of bad panels with gap mura defects. The unaccepted (bad) panels must be sorted out by experienced operators, and the production of unaccepted finished

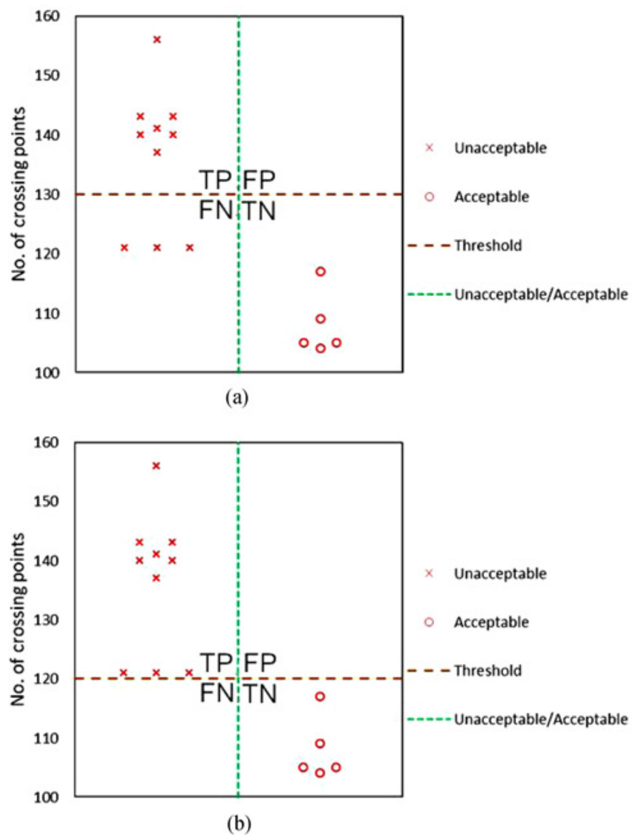

Fig. 8. Test results based on two different criteria. (a) Criterion 1: threshold = 130 points. (b) Criterion 2: threshold = 120 points.

TABLE III
COMPARISONS OF THE DIFFERENT METHODS OF INSPECTION

	Our method	Traditional method
Inspection time	< 2 seconds	10–20 seconds
Test method	Automatic visual detection	Detection by human eye
Test situation	Unfinished products (pre-test process)	Finished products
Test standard	Objective (base on gold standard)	Subjective
Cost saving	Good	Bad

panels will increase the cost of the product. The advantage of our proposed inspection procedure is that it takes place before the injection of liquid crystal into the panel. Defective panels can be sorted out beforehand to avoid wasting liquid crystal material. Furthermore, the test standard is objective and could quantize panels automatically. The disadvantage of our inspection procedure is that it can't detect other kinds of mura defects.

IV. CONCLUSION

The paper described a straightforward automatic quality control application for TFT LCD Panels. The described technique was based on automatic analysis of interference pattern fringes produced by TFT LCD panels when illuminated by a monochrome light source. The technique used image preprocessing, feature extraction, and a classification method based on a standard binary classification test.

Optical interference patterns and binary classification tests were used to speed up the pretest inspection process of TFT LCD panels for mura defects, especially for gap mura defects. Initial sorting by this method effectively reduced the cycle time on the production line (from 10-20 seconds per panel to less than two seconds). Thus, this method not only improved mura detection but also reduced the operators' work load. The computer aided method was less time-consuming than inspection by the human operator. In addition, the human eye got tired after a period of time and the operator was subject to error.

Although the optical interference technology and binary classification method were well known, the application discussed in this paper was new. The panel inspection method currently applied can only test finished LCD panels, it cannot prevent the production of bad panels. The advantage of this inspection procedure was that it took place before the injection of the liquid crystal into the panel. Defective panels can be sorted out, minimizing the waste of the liquid crystal material. The disadvantage of this inspection procedure was that we couldn't detect other kinds of mura defects. Results showed that our method can not only be used to find the gap mura defects but can also quantize panels automatically. The approach was simple but useful for automated visual inspection.

REFERENCES

[1] R. S. Chang, J. Z. Tsai, T. Y. Li, L. W. Ho, and C.F. Yang, "Pretest gap mura on TFT LCDs using the interference pattern method," in *Proc. IEEE/SICE Int. Symp. Syst.Integr. (SII)*, 2011, pp. 57–61.

[2] M. Mlejnek and A. Mafi, "Viewing angle and voltage dependence of the visibility of cell gap defects in LCD panels," *IEEE J. Disp. Technol.*, vol. 7, no. 12, pp. 684–687, Dec. 2011.

[3] W.-C. Li and D.-M. Tsai "Defect Inspection in low-contrast LCD images using hough transform-based nonstationary line detection," *IEEE Trans. Ind. Informat.*, vol. 7, no. 1, pp. 136–147, Feb. 2011.

[4] T. Asano, Y. Takagi, T. Kondo, J. Yao, and W. Liu, "Image quality evaluation based on human visual perception," in *Proc. IECON*, Nov. 2011, pp. 2141–2146.

[5] D. C. Tseng, Y. C. Lee, and C. E. Shie, "LCD mura detection with multi-image accumulation and multi-resolution background subtraction," *Int. J. Innovative Comput., Inf. Control*, vol. 8, no. 7(A), pp. 4837–4850, Jul. 2012.

[6] X. Bi, C. Zhuang, and H. Ding, "A new mura defect inspection way for TFT-LCD using level set method," *IEEE Signal Process. Lett.*, vol. 16, no. 4, pp. 311–314, Apr. 2009.

[7] K. Taniguchi, K. Ueta, and S. Tatsumi, "A detection method of mura on a coated layer using interference light," in *Proc. IEEE Int. Conf. SMC*, Taipei, Taiwan, 2006, pp. 5047–5052.

[8] C.-H. Oh, H. Joo, and K.-H. Rew, "Detecting low-contrast defect regions on glasses using highly robust model-fitting estimator," in *Proc. Int. Conf. Control, Autom. Syst.*, 2007, pp. 2138–2141.

[9] W.-H. Kao, J. C. Hung, and V. Hsu, "The MURA graphics problems in large area photomask for concept-based data mining techniques," in *Proc. Int. Conf. Ubi-Media Comput.*, 2008, pp. 490–495.

[10] H.W. Chow, N. C. Cheung, and W. Jin, "A low-cost submicrolinear incremental encoder based on 3×3 fiber-optic directional coupler," *IEEE Trans. Instrum. Meas.*, vol. 59, no. 6, pp. 1624–1633, Jun. 2011.

[11] M. Born, and E. Wolf, *Principles of Optics*, 7^{th} ed. Cambridge, U.K.: Cambridge Univ Ch.7, 1999.

[12] R. C. Gonzalez and R. E. Woods, *Digital Image Processing*, 2^{nd} ed. Upper Saddle, NJ, USA: Pearson/Prentice Hall, Ch. 3, 2008.

[13] G. Thomas, D. Flores-Tapia, and S. Pistorius," Histogram specification: A fast and flexible method to process digital images," *IEEE Trans. Instrum. Meas.*, vol. 60, no. 5, pp. 1565–1578, May 2011.

[14] K. Lee, Z. Man, D. Wang, and Z. Cao, "Classification of microarray datasets using finite impulse response extreme learning machine for cancer diagnosis," in *Proc. IECON*, Nov. 2011, pp. 2347–2352.

[15] C. Gao, L. Jian, S. Luo, "Modeling of the thermal state change of blast furnace hearth with support vector machines," *IEEE Trans. Ind. Electron.*, vol. 59, no. 2, pp. 1134–1145, Feb. 2012.

Jang-Zern Tsai received the B.S. degree in electrical engineering from National Central University, Jung-Li City, Taiwan, the M.S. degree in electrical engineering from National Tsing Hua University, Hsinchu, Taiwan, and the Ph.D. degree in electrical engineering from the University of Wisconsin-Madison, Madison, WI, USA.

He is Associate Professor of Electrical Engineering, National Central University, Jung-Li City, Taiwan. His current research interests include biochip design, biomedical instrumentation, biomedical signal processing, and bio-optics.

Rong-Seng Chang received the B.S. degree from the Department of Physics, Chung Cheng Institute of Technology, Daxi Township, Taiwan, the M.S. degree from the Department of Applied Physics, the Hebrew University of Jerusalem, Jerusalem, Israel, and the Ph.D. degree from the Optical Sciences Center, University of Arizona, Tucson, AZ, USA.

He is Professor of Optics and Photonics at National Central University, Jung-Li City, Taiwan. His current research interests include pattern recognition, optical systems, bio MEMS, nanotechnology, fuzzy systems and biochip design.

Tung-Yen Li received the B.S. degree from the Department of Electrical Engineering, National Taiwan Ocean University, Keelung, Taiwan, in 1999, the M.S degree from the Department of Optics and Photonics, National Central University, Jhong-Li, Taiwan, in 2002 and the Ph.D. degree in electrical engineering from National Central University, Taiwan in 2013.

His current research interests include electro-optics, and magnetic devices.